ACS APPLIED MATERIALS & INTERFACES

Research Article

www.acsami.org

Facile Method to Functionalize Graphene Oxide and Its Application to Poly(ethylene terephthalate)/Graphene Composite

Sang Hwa Shim,[†] Kyung Tae Kim,[†] Jea Uk Lee,[‡] and Won Ho Jo*,[†]

[†]WCU Hybrid Materials Program, Department of Materials Science and Engineering, Seoul National University, Seoul 151-742, Korea

[‡]Composite Materials Research Group, Korea Institute of Materials Science, Changwon, Gyeongnam, 642-831, Korea

Supporting Information

ABSTRACT: Graphene oxide (GO) prepared in bulk quantities by oxidation of graphite with strong oxidants contains many hydrophilic groups, such as hydroxyl, epoxy, and carboxyl acid. We present a method to efficiently convert these hydrophilic groups into alkyl and alkyl ether groups by a one step reaction of bimolecular nucleophilic substitution with alkyl bromide. The functionalized graphene oxide (fGO) can be homogeneously dispersed as exfoliated monolayers in various organic solvents without degradation of size and shape of graphene oxide sheet. The degree of substitution reaction of each hydrophilic group in GO with alkyl bromide is quantitatively determined by comparing the deconvoluted O 1s X-ray photoelectron spectrum of GO with that of fGO. Addition of a small amount of fGO in poly(ethylene terephthalate) (PET) improves remarkably tensile and gas barrier properties of PET/fGO composite due to homogeneous dispersion of fGO sheets in PET matrix.

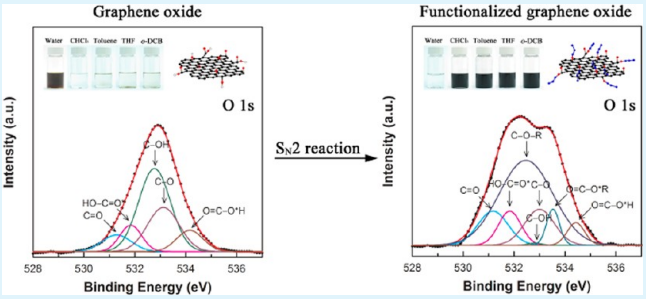

KEYWORDS: *functionalized graphene oxide, PET/fGO composite, mechanical property, gas barrier property*

1. INTRODUCTION

Graphene sheets, a single-atom-thick sheet of hexagonally arrayed sp^2-bonded carbon, have garnered tremendous interest because of their unique structure and outstanding physical properties such as high intrinsic carrier mobility,[1] tunable band gap,[2] high mechanical strength and elasticity,[3] and superior thermal conductivity.[4] These unique features of graphene sheets offer a wide variety of applications including nanoelectronics,[5,6] sensors,[7,8] capacitors,[9,10] and composite reinforcement.[11−14] For the pursuit of these applications, the development of a high-yield, high-throughput processing method for high quality graphene sheet would be exceptionally necessary. Thus, a number of studies for the fabrication of graphene sheets have been continuously reported.[15−19] Single-layer graphenes are directly obtained by a top-down approach (e.g., mechanical cleavage of graphite) and bottom-up approach (e.g., organic synthesis, epitaxial growth, and chemical vapor deposition). Although those routes might be preferred for precise device assembly with low defect, they can be less effective for large-scale manufacturing of graphene sheets.

Consequently, an alternative method for producing graphene sheets starting from graphene oxide (GO) has been suggested. The GO prepared in bulk quantities by oxidation of graphite with strong oxidants can be transformed back to graphene sheets by chemical,[20] thermal,[21] and electrochemical reduction.[22] Recently, this oxidation−reduction method to produce a graphene sheet from GO precursor has most widely been used, because this method is fast, simple, cost-effective, and largely scalable. Aside from a precursor of graphene sheet, GO itself also has several applications including polymer composite,[23,24] supercapacitor,[25] drug delivery,[26] hydrogen storage,[27] and organic photovoltaics.[28,29] However, owing to their hydrophilic nature, GO sheets are dispersed only in aqueous media that are incompatible with most of organic polymers.

Since graphenes dispersible in organic solvents have the potential to realize effective graphene-polymer composite, the development of organic soluble graphene has been beneficial. To date, the dispersion of graphene in organic solvents has been accomplished via covalent functionalization of GO sheets with several solvophilic groups: GO was modified by amidation reaction between the carboxyl acid group of GO and alkylamine,[30] by esterification between carboxylic acid group of GO and hydroxyl group in poly(vinyl alcohol),[31] by esterification between the carboxylic acid group of GO and ROH,[32] by Gomberg−Bachmann reaction between the aromatic ring and diazonium salt,[33] and by nucleophilic ring-opening reaction between the epoxy group of GO and amine group of an amine-terminated organic molecules.[34,35] The functionalized graphene sheets with solvophilic groups were well dispersed in polymer matrix, such as polycarbonate,[36] polyurethane,[37] and polystyrene,[38] and the composites showed enhanced mechanical properties and electrical conductivity.

Received: May 21, 2012
Accepted: July 5, 2012
Published: July 5, 2012

Scheme 1. Synthetic Procedure for Functionalization of GO

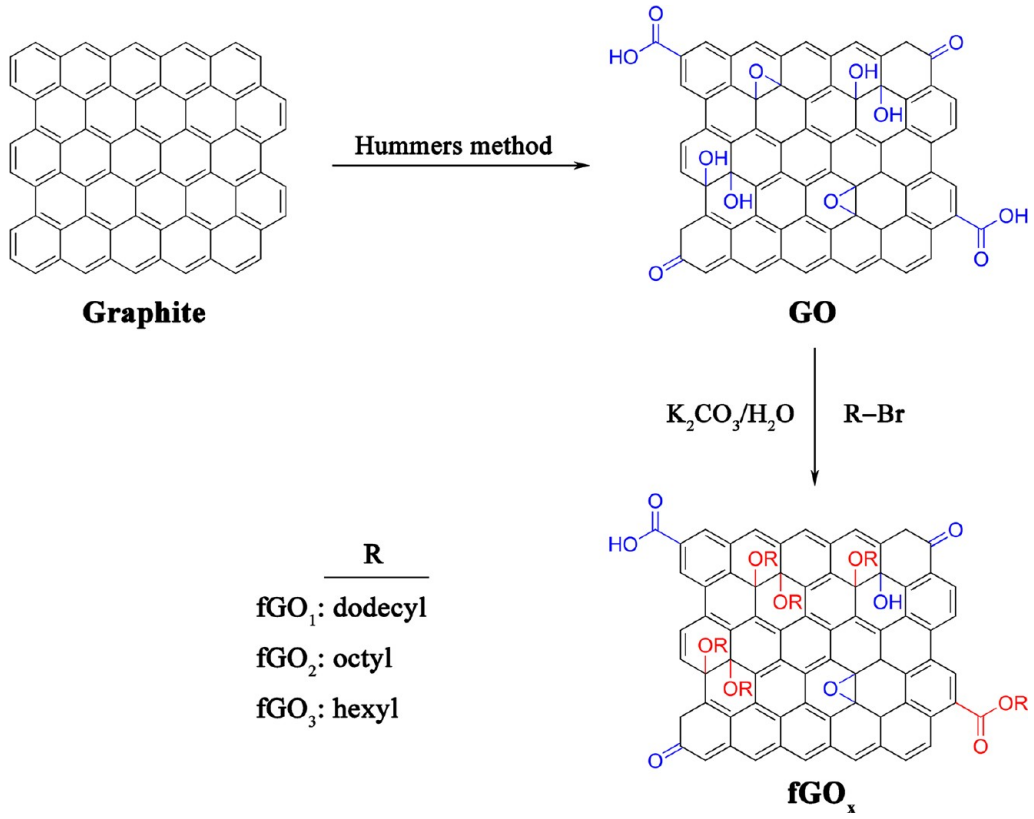

However, those functionalization methods neither are efficient nor produce highly soluble and long-term stable GO in various organic solvents.

Since poly(ethylene terephthalate) (PET) has good barrier properties against oxygen and carbon dioxide as well as good mechanical properties, it has been utilized in bottles and trays for various liquids and foods. However, these properties of PET should be further enhanced for high pressure bottles such as a carbonated beverage container. This enhancement would be achieved if graphenes could be homogeneously dispersed in PET because of inherent excellent mechanical properties and two-dimensional planar structure of graphenes.

In this paper, we report a new facile functionalization method of GO via bimolecular nucleophilic substitution (S_N2) reaction with alkyl bromide in a one step reaction, which is faster and simpler compared to other functionalization methods. Three kinds of alkyl groups (hexyl, octyl, and dodecyl) were introduced onto the graphene surface, and their dispersion in organic solvent is compared. The chemical structure of the functionalized graphene oxide (fGO) and the degree of functionalization are quantitatively identified using Fourier transform infrared (FT-IR), thermogravimetric analysis (TGA), and X-ray photoelectron spectroscopy (XPS). Finally, PET/fGO composites are prepared, and the mechanical and gas barrier properties of PET/fGO composites are examined in terms of the dispersion of fGO in PET matrix.

2. EXPERMENTAL SECTION

Synthesis of GO and fGOs. All reagents were purchased from Sigma Aldrich and were used without further purification. Graphite flake was oxidized by a modified Hummers method. In the pretreatment step that ensures complete oxidation, potassium persulfate (10 g) and phosphorus pentoxide (10 g) were added in sulfuric acid (50 mL) at 80 °C and stirred until the mixture was dissolved to prepare the oxidation solution. After graphite flake (10 g) was added to the oxidation solution and stirred at 80 °C for 4 h, the solution is diluted with 2 L of deionized (DI) water, stirred overnight, and filtered using ester cellulose membrane (Millipore, 0.2 μm pore size). The filtered mixture was washed with water to remove the oxidizing agents and dried in a vacuum oven.

Pretreated graphite (4 g), phosphorus pentoxide (62 g), and potassium manganate (24 g) were added to a solution of sulfuric acid (480 mL) and DI water (80 mL), and then, the mixed solution was stirred slowly for 12 h. After the solution was sonicated in a bath-type sonicator (Hwashin Instrument, Power Sonic 410) for 1 h, 35 wt % hydrogen peroxide (8 mL) and DI water (600 mL) were added to the solution. Thereafter, the mixed solution was stirred vigorously at room temperature and sonicated for 2 h once a day during 1 week. To dissolve nonreacted potassium manganate solid, 30% hydrogen chloride (300 mL) and ethanol (300 mL) were added to the reaction mixture. Then, the mixed solution was put into a metal sieve to sift out graphite. The filtered mixture was centrifuged at 7500 rpm for 1 h, and the supernatant was decanted away several times until pH of the supernatant was neutralized. The sediments were dried under vacuum overnight at room temperature. After GO (100 mg) and potassium carbonate (200 mg) were added in a mixture solvent of anhydrous dimethylformamide (25 mL) and water (2 mL), the solution was sonicated in a bath-type sonicator for 30 min and stirred at 100 °C for 12 h under nitrogen atmosphere. 1-Bromododecane (5.5 mL) was added to the mixed solution, and the solution was stirred at 100 °C for 48 h. The reaction solution was filtered by

dx.doi.org/10.1021/am300906z | ACS Appl. Mater. Interfaces 2012, 4, 4184–4191

PTFE membrane (Millipore, 0.45 μm pore size) and washed with chloroform, methanol, and DI water. The product (fGO_1) was dried at 30 °C in a vacuum oven. fGO_2 and fGO_3 were also prepared using bromooctane and bromohexane by the same procedure, respectively, as shown in Scheme 1.

Preparation of PET/fGO_1 Composite Films. All of PET/fGO_1 composites with different loadings of fGO_1 were prepared by solution blending. A typical procedure of PET/fGO_1 composite with 1 wt % of fGO_1 is as follows: A solution of 10 mg of fGO_1 in 5 mL of *o*-chlorophenol was sonicated for 1 h. The solution was then mixed with a solution of 1 g PET (Toray Saehan, M_w of 192 000) in 10 mL of *o*-chlorophenol. The mixture was sonicated for an additional 30 min and precipitated in excess methanol. The precipitate was collected by filtration and washed with methanol. The filter cake was dried at 70 °C for 24 h under vacuum.

Films of PET/fGO_1 composites were prepared by solution casting: A solution of PET/fGO_1 in *o*-chlorophenol was poured onto a glass plate, and then, a doctor blade was used to prepare a solution film. The solvent was slowly evaporated at room temperature for 24 h, and the resulting film was thoroughly dried under high vacuum at 70 °C for 24 h. For comparison, a film of PET/GO was also prepared by the same procedure.

General Characterization Methods. The functionalization of GO was identified by FT-IR (Thermo Scientific, Nicolet 6700). The dispersion state of GO and fGOs were observed by TEM (JEOL, JEM-1010), SEM (JEOL, JSM-7600F), and AFM (Surface imaging systems, NS4A). Thermal property was measured by TGA (TA Instruments, TGA 2050) under nitrogen atmosphere. The UV−visible absorption spectra of three fGOs in ortho-dichlorobenzene (*o*-DCB) were obtained from an UV−visible−NIR spectrophotometer (Perkin-Elmer, Lambda 25). X-ray photoelectron spectra were obtained on AXIS-His (Kratos).

The tensile properties of composite films were measured with a universal testing machine (Instron-5543, Instron) with a 1 KN load cell at a constant cross-head speed of 3 mm/min. At least five specimens were tested for each sample, and the tensile properties are reported on average. The crystallinity of PET and PET/fGO_1 were determined by measuring the heat of melting using a differential scanning calorimeter (DSC, TA Instruments). The gas barrier properties of composite films were measured using a gas permeation analyzer (MOCON, OX-TRAN 2/20).

3. RESULTS AND DISCUSSION

To disperse GO homogeneously in organic solvent such as tetrahydrofuran (THF), chloroform, and *o*-DCB, the hydrophilic groups in GO surface were converted to alkyl groups, as shown in Scheme 1. When GO was prepared via a modified Hummers method,[39] the GO sheets have three types of chemically reactive oxygens, viz. carboxylic acid, hydroxyl, and epoxy, which provide a reaction site for chemical modification. As the oxygen groups are reacted with alkylbromide in the presence of potassium carbonate, the oxygens of GO are first deprotonated to O^- or COO^- ions by potassium carbonate, and then, those are reacted with alkyl bromide by S_N2 reaction in one step to afford fGO.

The chemical structure of fGO_1 is identified by FT-IR spectroscopy, as shown in Figure 1. While the characteristic bands of GO are observed at 1050 and 3450 cm^{-1} (C−O and O−H stretching peak, respectively), 1702 cm^{-1} (C═O stretching in carboxylic acid group), 1230 cm^{-1} (C−O

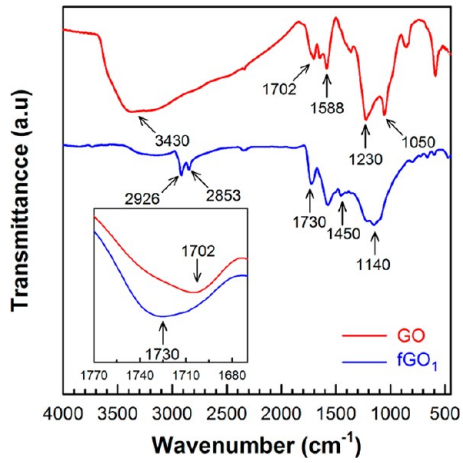

Figure 1. FT-IR spectra of GO and fGO_1. The inset shows the magnified spectra for C═O stretching vibrations of GO and fGO_1, indicating that the absorption band of carboxylic acid (1702 cm^{-1}) in GO shifts to that of ester (1730 cm^{-1}) in fGO_1.

stretching in epoxy group), and 1588 cm^{-1} (C═C stretching), new peaks are observed in the spectrum of fGO_1 at 1140, 2853, and 2926 cm^{-1}, corresponding to C−O−C bending and C−H stretching vibrations in the substituted alkyl group, respectively, and concomitantly, the peaks at 1050 cm^{-1}, 1230 cm^{-1} (C−O stretching in hydroxyl and epoxy groups), and 3430 cm^{-1} (O−H stretching) are largely decreased, indicating that most of the hydroxyl and epoxy groups are converted to ether groups by the substitution reaction. The carboxylic acid groups (1702 cm^{-1}) in GO are also partially changed to the ester group (1730 cm^{-1}), as shown in the inset of Figure 1. This observation demonstrates that hydroxyl, epoxy, and carboxylic acid groups of GO are substituted with alkyl groups. FT-IR spectra of fGO_2 and fGO_3 also show the same feature as that of fGO_1 (see Figure S1, Supporting Information). Raman spectrum and TGA thermogram also support the modification of GO, because the C−C stretching peak (1150 cm^{-1}) of dodecyl group appears in the Raman spectrum of fGO_1 while the C−C stretching peak is not observed in the Raman spectrum of GO (Figure S2, Supporting Information), and the weight loss of fGO_1 exhibits different behavior from that of GO (Figure S3, Supporting Information). In addition, EDS spectra provide another evidence for the successful substitution of GO because the carbon/oxygen ratio of fGO_1 is higher than that of GO and the Br peak is absent in the EDS spectrum of fGO_1 (see Figure S4, Supporting Information).

To examine the solubility of fGO_1 in organic solvents, the dispersions of GO and fGO_1 in organic solvents are compared (see Figure S5, Supporting Information). GO is readily dispersed in water due to the presence of hydrophilic groups, whereas it is not dispersed in organic solvents such as chloroform, toluene, THF, and *o*-DCB. In contrast with GO, fGO_1 is homogeneously dispersed in various organic solvents while it is precipitated in water. Especially, the dispersion of fGO_1 in *o*-DCB was stable for several weeks standing. This result clearly indicates that substituted alkyl groups in fGO_1 change the surface property of GO.

The exfoliation state of GO in water and fGO_1 in organic solvent (*o*-DCB) was identified by TEM, as shown in Figure 2. While GO is well dispersed in water as single layers,[40] fGO_1 is homogeneously dispersed in *o*-DCB as single layers without degradation of size of the graphene sheet by the substitution

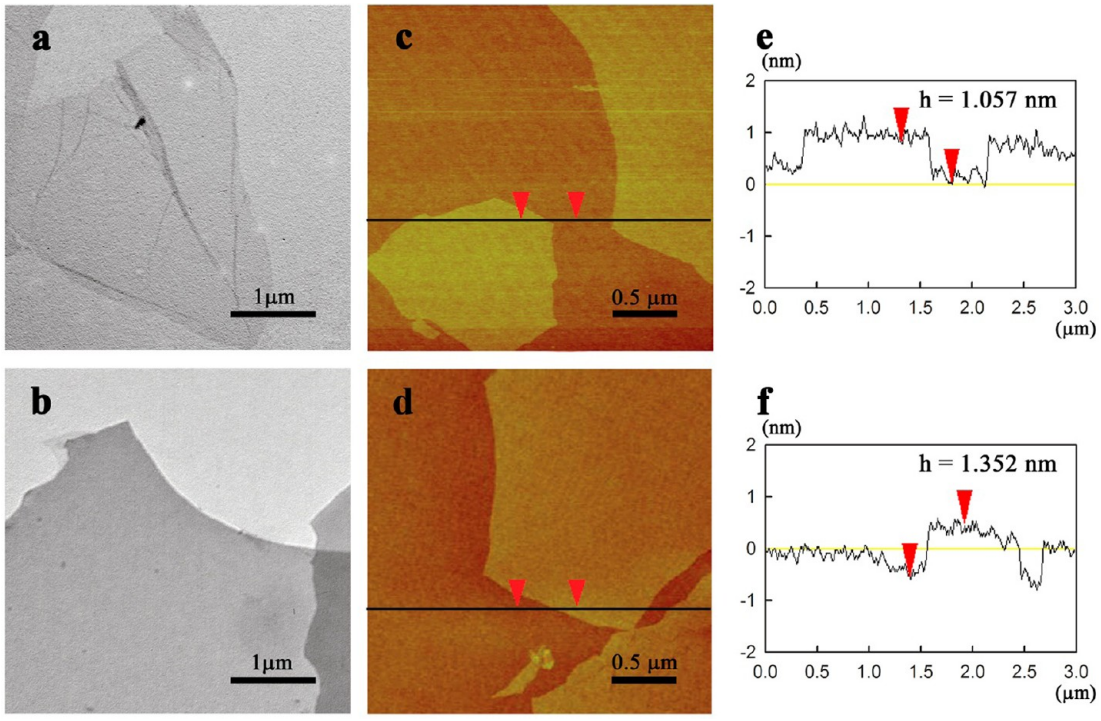

Figure 2. TEM images of (a) GO and (b) fGO_1; AFM images of (c) GO and (d) fGO_1, and height profiles of (e) GO and (f) fGO_1.

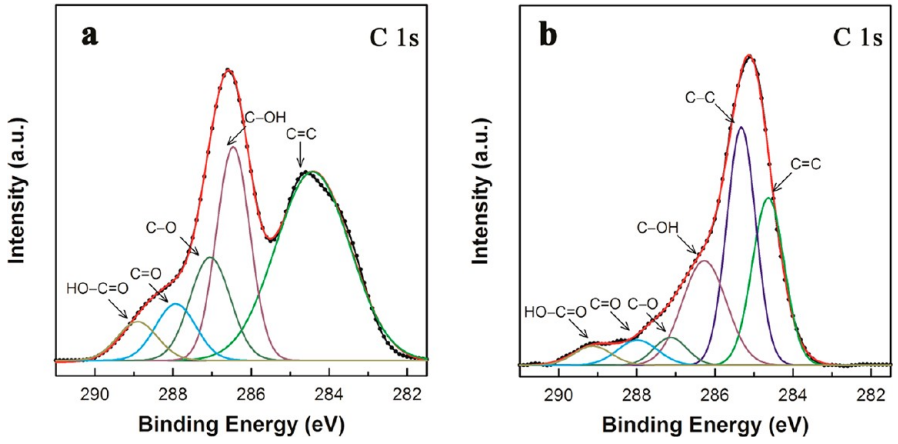

Figure 3. The C1s XPS spectra of (a) GO and (b) fGO_1 with deconvoluted peaks.

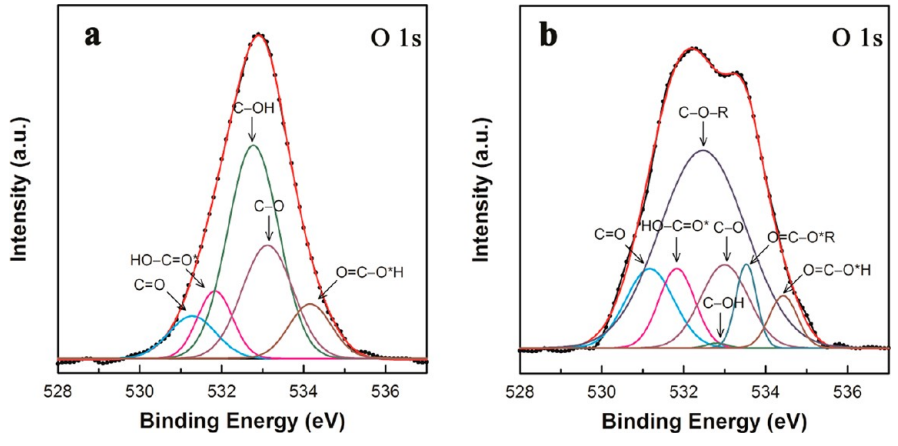

Figure 4. The O1s XPS spectra of (a) GO and (b) fGO_1 with deconvoluted peaks.

dx.doi.org/10.1021/am300906z | ACS Appl. Mater. Interfaces 2012, 4, 4184–4191

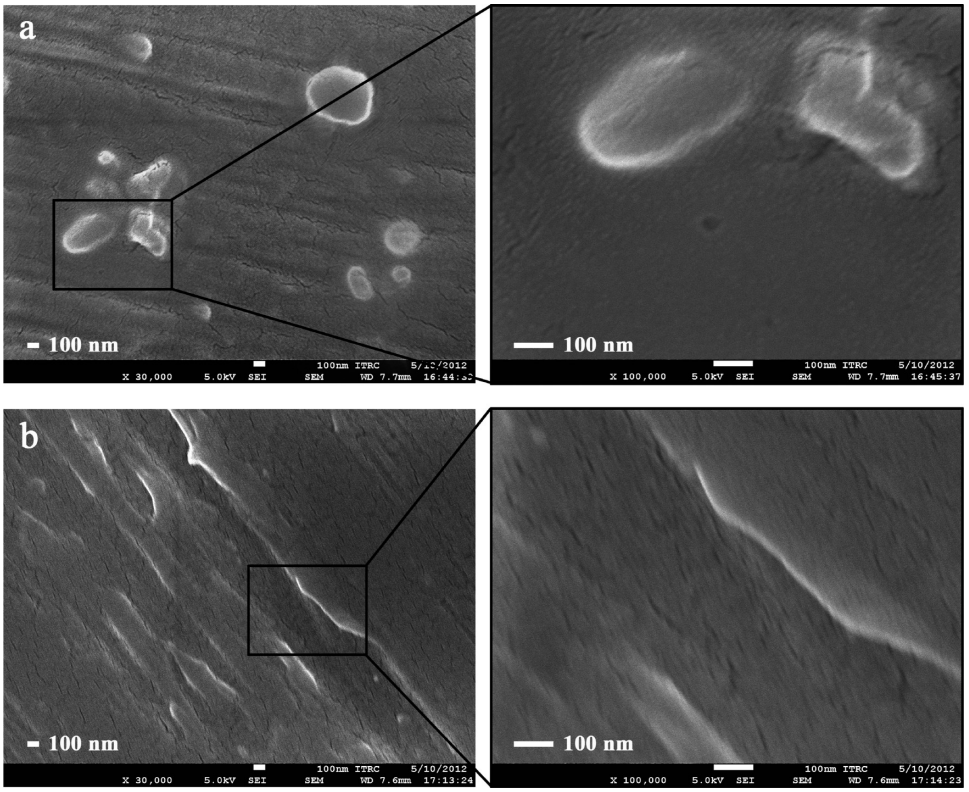

Figure 5. SEM images of PET/GO (a) and PET/fGO_1 (b) composites with 1 wt % GO and fGO_1. Right side images are magnified ones.

reaction. The surface images and height profiles of AFM for GO and fGO_1 also reveal that the individual graphene sheets remain exfoliated after functionalization (Figure. 2). The AFM images of GO in water and fGO_1 in *o*-DCB show the existence of irregularly shaped sheets with uniform thickness and lateral dimension of a few micrometers. The height profiles along the straight line depicted in Figure 2c,d show that the height of GO is about 1 nm, consistent well with the reported value[41] (Figure 2e) while the height of fGO_1 is in the range of 1.3−1.5 nm, which is obviously larger than that of GO due to the introduction of alkyl groups on the surface of GO (Figure 2f). The above result indicates that our functionalization method is very effective to obtain functionalized individual graphene sheets.

Although it was qualitatively identified by FT-IR that hydroxyl, epoxy, and carboxylic acid groups in GO are converted to ether and ester linkages by the substitution reaction, we analyzed and compared the C 1s and O 1s XPS spectra of GO and fGO for quantitative analysis of the substitution reaction, as shown in Figures 3 and 4, respectively. Figure 3a shows the C 1s XPS spectrum of GO which can be deconvoluted into five components: C═C (284.5 eV), C−OH (286.4 eV), C−O (epoxy) (287.1 eV), C═O (288.0 eV), and C═O(OH) (289.2 eV),[42−44] while the C 1s signal of f-GO_1 exhibits an additional new peak at 285.3 eV corresponding to C−C sp^3 carbon due to alkyl groups in fGO, as shown in Figure 4b. Since the C 1s peaks of ether and ester in fGO_1 have the same positions as those of hydroxyl (C−OH) and carboxylic acid in GO, respectively, it is not possible to analyze quantitatively the degree of reaction from those peaks. Nevertheless, the comparison of C 1s spectra of GO and fGO indicates that a considerable amount of hydrophilic groups in GO was replaced by alkyl group, because the peak intensity of hydrophilic groups is significantly decreased except the hydroxyl group and concomitantly the new peak of alkyl group is observed at 285.3 eV in fGO_1 (Figure 3 and Table S1, Supporting Information). The atomic percentages of various type of carbons in GO and fGOs are determined from the deconvoluted XPS spectra and listed in Table S1, Supporting Information.

For quantitative analysis of the degree of substitution reaction, we analyzed the O 1s XPS spectra of GO and fGOs. The binding energies of oxygens in various functional groups were assigned according to the literature,[45−48] as shown in Figure 4. Since the hydroxyl and epoxy groups in GO are converted to ether linkages and a considerable amount of carboxylic acid groups are converted to ester linkages after the substitution reaction, the XPS spectrum of fGO shows two additional peaks at 532.6 and 533.6 eV, which correspond to oxygens of C−O−R (ether) and O═C−O*R (ester), respectively. The O 1s peak positions and their relative atomic percentages are listed in Table S2, Supporting Information. When the atomic percentages of oxygens in GO are compared with those in fGO_1, it reveals that 99% of C−OH (hydroxyl) and 53% of C−O (epoxy) are converted to C−O−R and that 43% of O═C−OH (carboxylic acid) is also converted to O═C−OR (ester). It should be noted that the conversion from carboxylic acid to ester (10.6−4.7 = 5.9%) is almost consistent with the atomic percentage of ester in fGO_3 (5.5%) within a deconvolution error. Furthermore, the amount of ether linkage in fGO_1 (53.9%) is also nearly consistent with the sum of the conversion from hydroxyl (45.2 − 0.3 = 44.9%) and the conversion from epoxy (24.0−12.8 = 11.2%). fGO_2 and fGO_3 also show similar behavior to fGO_1 (see Table S2 and Figure S6, Supporting Information), indicating that the substitution reaction is not dependent upon the chain length of alkyl

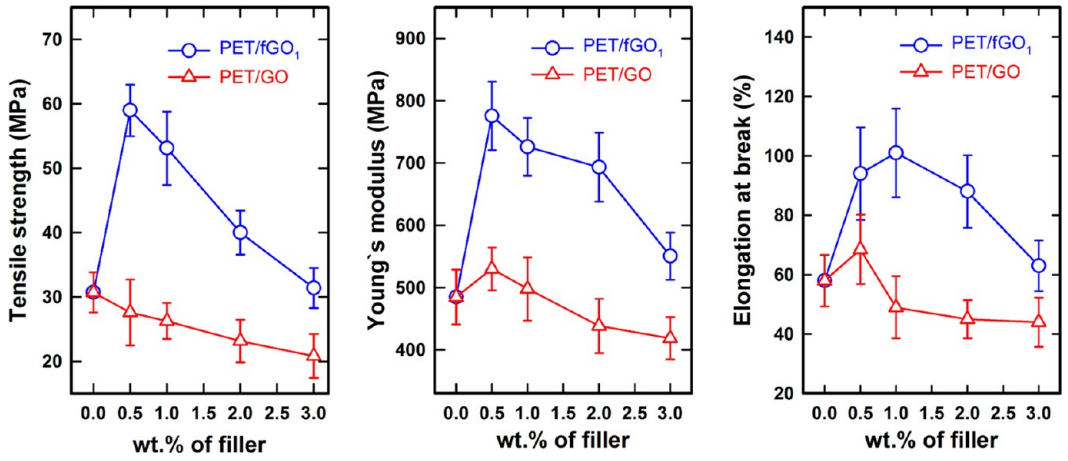

Figure 6. Mechanical properties of PET/fGO_1 (red △) and PET/GO (blue ○) composites as a function of GO and fGO_1 content.

bromide. In short, most of the hydroxyl groups in GO are reacted with alkyl bromide while about half of epoxy and carboxylic acid in GO are converted to ether and ester by the substitution reaction, respectively.

The effect of alkyl chain length on the dispersion of fGOs in organic solvent (*o*-DCB) was examined by comparing UV−vis absorptions of three fGO solutions (Figure S7, Supporting Information). Since the absorption coefficients of three fGOs are equal (Figure S8, Supporting Information), the absorbance of each solution is proportional to the dispersed concentration of fGO in solution. Hence, the largest absorption of fGO_1 indicates that the dodecyl group in fGO_1 affords the best dispersing ability in *o*-DCB.

The homogeneous dispersion of filler in composite is one of the most important requirements to effectively enhance the matrix properties. When the dispersion of GO and fGO in PET matrix was examined by SEM images, as shown in Figure 5, it revealed that GO sheets in PET/GO composite were rolled to minimize the contact area with immiscible PET matrix and aggregated with uneven distribution of GOs in PET matrix, whereas fGOs in PET/fGO composite were homogenously dispersed with individually exfoliated fGO_1 sheets in PET matrix, indicating that the alkyl groups in fGO_1 improve the compatibility between PET and fGO_1.

When the tensile properties of neat PET, PET/GO, and PET/fGO_1 were plotted against GO and fGO_1 loading, as shown in Figure 6 and Figure S9, Supporting Information, tensile properties of PET/GO composites were inferior to those of neat PET, while both tensile strength and Young's modulus of PET/fGO_1 were superior to those of neat PET. The negative behavior of PET/GO is mainly attributed to poor dispersion of GO in PET matrix (Figure 5a) whereas the enhancement of tensile properties of PET/fGO_1 may arise from good interfacial adhesion between fGO_1 and PET owing to preferential interaction between the alkyl groups in fGO_1 and PET matrix. However, when the addition of fGO_1 exceeds 1 wt % addition, the mechanical properties of the composite start to decrease, showing the maximum at 0.5 wt % addition. The reason for this decrease is probably due to some aggregation of fGO_1 sheets in PET matrix when more than 1 wt % of fGO_1 is added (see Figure S10, Supporting Information). Another interesting feature of mechanical properties is that the elongation-at-break of PET/fGO_1 increases with addition of fGO_1 in PET matrix (Figure 6). This is not a usual case, because it has been known that the elongation-at-break of most composites decreases with addition of fillers while the modulus of the composites increases. The increase of elongation-at-break in PET/fGO_1 is probably because the fillers (fGO_1) suppress stress-induced crystallization as the fillers act to disrupt the formation of crystalline lattice by their physical presence.[49] To identify the effect of fGO_1 on the crystallization of PET, the crystallinity of PET composite was measured before and after stretching by DSC (see Figure S11 and Table S3, Supporting Information). The crystallinities of neat PET and PET/fGO_1 films were 14.6% and 14.1% before stretching, respectively, while the crystallinities of the two films increased up to 19.5% and 16.7%, respectively, after stretching until breaking, indicating that the stretching-induced crystallinity of PET/fGO_1 composite was smaller than that of neat PET. This suppression of strain induced crystallization in PET/fGO_1 makes the PET matrix more ductile and as a result increases the elongation-at-break.

The gas barrier properties of neat PET, PET/GO, and PET/fGO_1 were measured by a gas permeation analyzer. Oxygen permeability coefficient (P) in Barrer unit (1 Barrer = 10^{-10} $cm^2/s{\cdot}cmHg$) is expressed as $P = (OTR{\cdot}t)/\Delta p$ where OTR is the equilibrium oxygen transmission rate of film, t is the film thickness, and Δp is the pressure gradient across the membrane. When the oxygen permeability coefficients of PET, PET/GO (1 wt %), and PET/fGO_1 (1 wt %) are compared, as shown in Figure 7, it reveals that the oxygen permeability coefficients of PET/GO and PET/fGO_1 are decreased by 38% and 85% as compared to that of neat PET, respectively. Especially, the oxygen permeability of PET/fGO_1 (3 wt %) was reduced by about 96% compared to that of neat PET, indicating that the oxygen permeability of fGO_1 is reduced more effectively than that of GO due to homogeneous dispersion and 2-dimensional planar structure of graphene in PET matrix.

4. CONCLUSIONS

We have proposed a versatile and facile functionalization method of GO with alkylbromide by S_N2 reaction. All functional groups in GO, such as hydroxyl, epoxy, and carboxylic acid are easily reacted with alkylbromide in a one-step reaction, and the degree of substitution reaction of each group is quantitatively determined by comparing the O1s XPS spectrum of GO with those of fGOs. fGOs are homogeneously dispersed in several organic solvents. Addition of a small amount of fGO in PET matrix improves remarkably the tensile

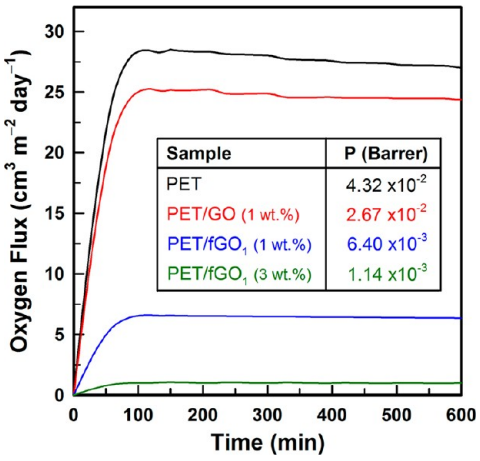

Figure 7. Oxygen flux rate and oxygen permeability coefficient of PET, PET/GO, and PET/fGO$_1$.

and gas barrier properties due to homogeneous dispersion of graphene sheets in PET matrix. This functionalization method can be used for many other applications, because any specific functional compounds with alkyl-bromide moiety can be covalently bonded onto the GO surface by a simple S_N2 reaction.

■ ASSOCIATED CONTENT

Supporting Information

FT-IR spectra of fGOs, EDS spectra, TGA thermogram, XPS analysis, UV−vis absorption spectra, absorption coefficient, stress−strain curve of composites, SEM image, DSC thermograms, and table of crystallinity data. This material is available free of charge via the Internet at http://pubs.acs.org.

■ AUTHOR INFORMATION

Corresponding Author

*E-mail: whjpoly@snu.ac.kr. Tel.:+82-2-880-7192. Fax: +82-2-876-6086.

Notes

The authors declare no competing financial interest.

■ ACKNOWLEDGMENTS

The authors thank the Ministry of Education, Science and Technology (MEST), Korea, for financial support through the Global Research Laboratory (GRL) and the World Class University (WCU) programs.

■ REFERENCES

(1) Morozov, S. V.; Novoselov, K. S; Katsnelson, M. I; Schedin, F.; Elias, D. C.; Jaszczak, J. A.; Geim, A. K. *Phys. Rev. Lett.* **2008**, *100*, 016602.
(2) Zhang, Y. B.; Tang, T. T.; Girit, C.; Hao, Z.; Martin, M. C.; Zettl, A.; Crommie, M. F.; Shen, Y. R.; Wang, F. *Nature* **2009**, *459*, 820−823.
(3) Lee, C.; Wei, X. D; Kysar, J. W.; Hone, J. *Science* **2008**, *321*, 385−388.
(4) Balandin, A. A; Ghosh, S.; Bao, W. Z; Calizo, I.; Teweldebrhan, D.; Miao, F.; Lau, C. N. *Nano Lett.* **2008**, *8*, 902−907.
(5) Berger, C.; Song, Z.; Li, T.; Li, X.; Ogbazghi, A. Y.; Feng, R.; Dai, Z. T.; Marchenkov, A. N.; Conrad, E. H.; First, P. N; Heer, W. A. *J. Phys. Chem. B* **2004**, *108*, 19912−19916.
(6) Westervelt, R. M. *Science* **2008**, *320*, 324−325.
(7) Ang, P. K.; Chen, W.; Wee, A. T. S.; Loh, K. P. *J. Am. Chem. Soc.* **2008**, *130*, 14392−14393.
(8) Robinson, J. T.; Perkins, F. K.; Snow, E. S.; Wei, Z. Q.; Sheehan, P. E. *Nano Lett.* **2008**, *8*, 3137−3140.
(9) Stoller, M. D.; Park, S. J.; Zhu, Y. W.; An, J. H.; Ruoff, R. S. *Nano Lett.* **2008**, *8*, 3498−3502.
(10) Wang, Y.; Shi, Z. Q.; Huang, Y.; Ma, Y. F; Wang, C. Y.; Chen, M. M.; Chen, Y. S. *J. Phys. Chem. C* **2009**, *113*, 13103−13107.
(11) Stankovich, S.; Dikin, D. A.; Dommett, G. H. B.; Kohlhaas, K. M.; Zimney, E. J; Stach, E. A.; Piner, R. D.; Nguyen, S. T.; Ruoff, R. S. *Nature* **2006**, *442*, 282−286.
(12) Yang, X.; Tu, Y.; Shang, S.; Tao, X. *ACS Appl. Mater. Interface* **2010**, *2*, 1707−1713.
(13) Vickery, J. L.; Patil, A. J.; Mann, S. *Adv. Mater.* **2009**, *21*, 2180−2184.
(14) Prasad, K. E.; Das, B.; Maitra, U.; Ramamurty, U.; Rao, C. N. R. *Proc. Natl. Acad. Sci. U.S.A.* **2009**, *106*, 13186−13189.
(15) Rao, C. N. R.; Sood, A. K.; Voggu, R.; Subrahmanyam, K. S. *J. Phys. Chem. Lett.* **2010**, *1*, 572−580.
(16) Geim, A. K.; Novoselov, K. S. *Nat. Mater.* **2007**, *6*, 183−191.
(17) Wu, J. S.; Pisula, W.; Mullen, K. *Chem. Rev.* **2007**, *107*, 718−747.
(18) Berger, C.; Song, Z.; Li, X.; Wu, X.; Brown, N.; Naud, C.; Mayou, D.; Li, T.; Hass, J.; Marchenkov, A. N.; Conrad, E. H.; First, P. N.; Heer, W. A. *Science* **2006**, *312*, 1191−1196.
(19) Kim, K. S.; Zhao, Y.; Jang, H.; Lee, S. Y.; Kim, J. M.; Ahn, J. H.; Kim, P.; Choi, J. Y.; Hong, B. H. *Nature* **2009**, *457*, 706−710.
(20) Park, S.; Ruoff, R. S. *Nat. Nanotechnol.* **2009**, *4*, 217−724.
(21) McAllister, M. J.; Li, J. L.; Adamson, D. H.; Schniepp, H. C.; Abdala, A. A.; Liu, J.; Herrera-Alonso, M.; Milius, D. L.; Car, R.; Prud'homme, R. K.; Aksay, I. A. *Chem. Mater.* **2007**, *19*, 4396−4404.
(22) Sundaram, R. S.; Gomez-Navarro, C.; Balasubramanian, K.; Burghard, M.; Kern, K. *Adv. Mater.* **2008**, *20*, 3050−3053.
(23) Fang, M.; Wang, K. G.; Lu, H. B.; Yang, Y. L.; Nutt, S. *J. Mater. Chem.* **2009**, *19*, 7098−7105.
(24) Layek, R. K.; Samanta, S.; Chatterjee, D. P.; Nandi, A. K. *Polymer* **2010**, *51*, 5846−5856.
(25) Wang, H.; Hao, Q.; Yang, X.; Lu, L.; Wang, X. *ACS Appl. Mater. Interfaces* **2010**, *2*, 821−828.
(26) Sun, X. M.; Liu, Z.; Welsher, K.; Robinson, J. T.; Goodwin, A.; Zaric, S.; Dai, H. J. *Nano Res.* **2008**, *1*, 203−212.
(27) Wang, L.; Lee, K.; Sun, Y. Y.; Lucking, M.; Chen, Z. F.; Zhao, J. J.; Zhang, S. B. B. *ACS Nano* **2009**, *3*, 2995−3000.
(28) Li, S. S.; Tu, K. H.; Lin, C. C.; Chen, C. W.; Chhowalla, M. *ACS Nano* **2010**, *4*, 3169−3174.
(29) Liu, Z. F.; Liu, Q.; Huang, Y.; Ma, Y. F.; Yin, S. G.; Zhang, X. Y.; Sun, W.; Chen, Y. S. *Adv. Mater.* **2008**, *20*, 3924−3930.
(30) Niyogi, S.; Bekyarova, E.; Itkis, M. E.; McWilliams, J. L.; Hamon, M. A.; Haddon, R. C. *J. Am. Chem. Soc.* **2006**, *128*, 7720−7721.
(31) Veca, L. M.; Lu, F. S.; Meziani, M. J.; Cao, L.; Zhang, P. Y.; Qi, G.; Qu, L. W.; Shrestha, M.; Sun, Y. P. *Chem. Commun.* **2009**, 2565−2567.
(32) Salavagione, H. J.; Gomez, M. A.; Martinez, G. *Macromolecules* **2009**, *42*, 6331−6334.
(33) Zhong, Z.; Dai, Y.; Ma, D.; Wang, Z. Y. *J. Mater. Chem.* **2011**, *21*, 6040−6045.
(34) Yang, H. F.; Shan, C. S.; Li, F. H.; Han, D. X.; Zhang, Q. X.; Niu, L. *Chem. Commun.* **2009**, 3880−3882.
(35) Wang, S.; Chia, P. J.; Chua, L. L.; Zhao, L. H.; Png, R. Q.; Sivaramakrishnan, S.; Zhou, M.; Goh, R. G. S.; Friend, R. H.; Wee, A. T. S.; Ho, P. K. H. *Adv. Mater.* **2008**, *20*, 3440−3446.
(36) Kim, H.; Macosko, C. W. *Polymer* **2009**, *50*, 3797−3809.
(37) Kim, H.; Miura, Y.; Macosko, C. W. *Chem. Mater.* **2010**, *22*, 3441−3450.
(38) Compton, O. C.; Kim, S.; Pierre, C.; Torkelson, J. M.; Nguyen, S. T. *Adv. Mater.* **2010**, *22*, 4759−4763.
(39) Hummers, W. S.; Offeman, R. E. *J. Am. Chem. Soc.* **1958**, *80*, 1339.
(40) He, H. K.; Gao, C. *Chem. Mater.* **2010**, *22*, 5054−5064.

(41) Marcano, D. C.; Kosynkin, D. V.; Berlin, J. M.; Sinitskii, A.; Sun, Z. Z.; Slesarev, A.; Alemany, L. B.; Lu., W.; Tour, J. M. *ACS Nano* **2010**, *4*, 4806−4814.
(42) Mattevi, C.; Eda, G.; Agnoli, S.; Miller, S.; Mkhoyan, K. A.; Celik, O.; Mostrogiovanni, D.; Granozzi, G.; Garfunkel, E.; Chhowalla, M. *Adv. Funct. Mater.* **2009**, *19*, 2577−2583.
(43) Liu, F.; Seo, T. S. *Adv. Funct. Mater.* **2010**, *20*, 1930−1936.
(44) Compton, O. C.; Dikin, D. A.; Putz, K. W.; Brinson, L. C.; Nguyen, S. T. *Adv. Mater.* **2010**, *22*, 892.
(45) Briggs, D.; Beamson, G. *Anal. Chem.* **1993**, *65*, 1517−1523.
(46) Mahl, S.; Lachnitt, J.; Niemann, R.; Neumann, M.; Baalmann, A.; Kruse, A.; Schlett., V. *Surf. Interface Anal.* **1996**, *24*, 405−410.
(47) Jama, C.; Dessaux, O.; Goudmand, P.; Gengembre, L.; Grimblot, J. *Surf. Interface Anal.* **1992**, *18*, 751−756.
(48) Stobinski, L.; Lesiak, B.; Zemek, J.; Jiricek, P.; Biniak, S.; Trykowski, G. *J. Alloys Compd.* **2010**, *505*, 379−384.
(49) Taniguchi, A.; Cakmak, M. *Polymer* **2004**, *45*, 6647−6654.